WATER RESOURCES RESEARCH, VOL. 33, NO. 1, PAGES 13–19, JANUARY 1997

Electrical structure beneath the eastern collapsed flank of Piton de la Fournaise volcano, Reunion Island: Implications for the quest for groundwater

Marc Descloitres and Michel Ritz

Institut Français de Recherche Scientifique pour le Developpement en Coopération, Dakar, Senegal

Bernard Robineau and Michel Courteaud

Laboratoire des Sciences de la Terre, Université de la Réunion, Ile de la Reunion, France

Abstract. Time domain electromagnetic (TDEM) and tensor audiomagnetotelluric (AMT) data have been acquired at several locations on the eastern flank of Piton de la Fournaise volcano (Reunion Island) within a depressed area called Grand Brulé, interpreted as a collapse structure. The survey objectives were (1) to provide a geophysical estimate of the subsurface structure and (2) to evaluate the possibility of detecting aquifers in a volcanic environment not very known. The TDEM and the AMT data collected along two E-W traverses orthogonal to coastline on the northern and southern edges of Grand Brulé were interpreted with one-dimensional layered models. From the surface downward, the geoelectrical sections reveal two major units: very resistive, young lava flows (dry) and a shallow conductor (<500 m) which is probably primarily attributable to a clayey, poorly permeable base. A notable exception to this pattern is seen at sites close to the coast, where we found three-layered structures. There is an intermediate layer of resistivity of about 100–200 ohm m between the top resistive layer and bottom conductive layer that represents a probable freshwater lens in the southern part and an alluvial fan with resistivities substantially higher (200 ohm m) in the northern part of Grand Brulé. It is suggested that the 200 ohm m layer, interpreted as a buried paleoriver, corresponds to a drainage structure.

Introduction

Electrical geophysical techniques are tools suited to groundwater exploration in coastal and island regions because the resistivity of water-bearing rocks is strongly dependent on the water content, the water salinity, and the manner in which the water is distributed throughout the rock [*Keller and Frischknecht*, 1966]. These methods are applicable mostly in shallow aquifers where contrasts in resistivity might be expected.

As part of the Fournaise Massif (Reunion Island) hydrogeological research program, a survey with audiomagnetotelluric (AMT) and time domain electromagnetic (TDEM) methods was carried out in the Grand Brulé (GB) area (Figure 1) on the east flank of the Piton de la Fournaise active shield volcano. The TDEM center loop sounding method was selected because of its good lateral resolution, and AMT method was initiated for detection of deeper structures compared to TDEM soundings.

The main objectives of the survey were to establish the resistivity stratification with depth, to identify formations with anomalous electrical properties, and to attempt to correlate these formations with areas where water will be predominantly flowing. The choice of sites was intended to provide two radial profiles across the Grand Brulé. The ability to follow this criterion was considerably affected by geographic factors. To the east, access problems limited the choice of sites because of rugged topography above 800-m elevations. Finally, TDEM/AMT soundings were obtained at 14 sites (Figure 1) along the northern and southern edges of Grand Brulé. When the electromagnetic methods are applied to investigate such a volcanic area, surface topography and near-surface conductive features also complicate the interpretation [*Wannamaker et al.*, 1986; *Eaton and Hohmann*, 1987]. However, topographic effects for a slope in AMT [*Wannamaker et al.*, 1986] appear relatively weak if breaks in slope are not large, and the AMT response may be obtained accurately. In this paper we report the results of TDEM and AMT soundings. We present results for the Grand Brulé geophysical survey as two-dimensional (2-D) cross sections made from pieced together one-dimensional (1-D) models. These results are then discussed.

Grand Brulé represents the coastal part of a peculiar morphological feature on the eastern part of Piton de la Fournaise. This U-shaped feature, bordered by two linear cliffs and interpreted as a collapse structure, opens the caldera to the ocean. Its surface is covered by recent low-dipping basaltic lava overflowing from the caldera. Previous interpretations of a huge slumped block [*Duffield et al.*, 1982] or multiple landslides on the volcano eastern flank [*Chevallier and Bachèlery*, 1981] have recently been discussed after oceanographic surveys and large debris slumps have been mapped just offshore Grand Brulé [*Lénat et al.*, 1989]. A reconnaissance AMT survey was carried out by *Benderitter and Gérard* [1984] across Grand Brulé. Results showed a conductive layer at depths of 0.5–1 km beneath the northern coastal part of Grand Brulé and Bois Blanc rampart area. A gravimetric survey has revealed a major anomaly

Paper number 96WR02673.
0043-1397/97/96WR-02673$09.00

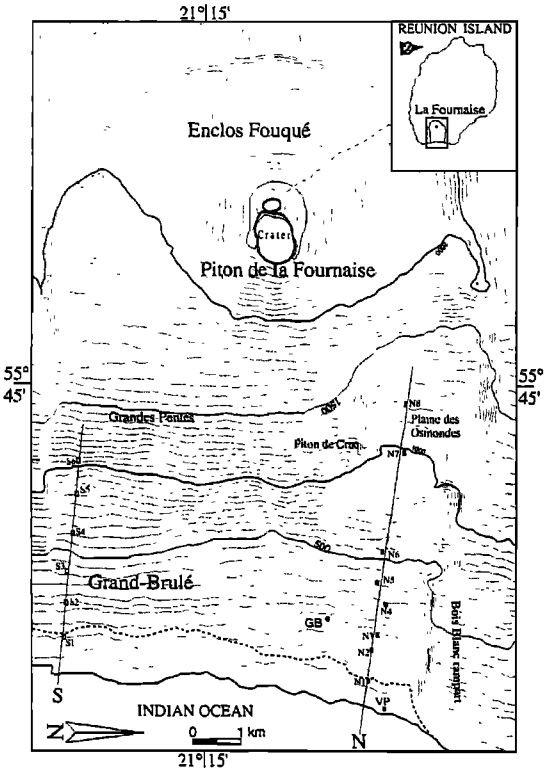

Figure 1. Map of survey area showing the location of the tensor audiomagnetotelluric (AMT)/time domain electromagnetic (TDEM) soundings with their site number. Also shown is the location of the Vierge au Parasol (VP) and Grand Brulé (GB) geothermal drillholes. Lines N and S are the locations of the cross sections shown in Figure 4. The elevation contours are in meters. The inset map shows the location of survey area in Reunion Island.

in the lower part of Grand Brulé, modeled as a dense elliptic intrusive body that has been found 800 m below sea level (BSL) by a deep geothermic exploration drilling [*Rançon et al.*, 1989].

TDEM Soundings

Field measurements were made with the time domain electromagnetic Geonics EM47 system using a controlled-current source attached to a square transmitter loop of 100 m × 100 m. A multiturn air coil receiver is placed in the center of the loop. The array is relocated for each sounding. The current waveform driven through the transmitter loop consists of equal periods of time-on and time-off. The transient response is created by abruptly turning off the current in the transmitter loop. An apparent resistivity is calculated as a function of time after the current turn-off [*Kaufman and Keller*, 1983; *Fitterman and Stewart*, 1986]. With increasing time the induced currents have reached further into the formation and hence, are representative of greater depths. The relationship between time and depth is influenced by the distribution of electrical resistivities in the earth. The field data acquired were then interpreted with layered models using the TEMIXGL (Interpex Ltd.) interpretation package to obtain a solution for the resistivity stratification of the subsurface.

Figure 2 shows some representative TDEM soundings performed over the northern (sites N5 and N8) and southern (site S1) edges of Grand Brulé (Figure 1). The quantitative interpretation of TDEM data is hampered by the principle of equivalence, which means that many different layered models may produce practically the same resistivity curve. The data were interpreted with the minimum number of layers that gave a good fit. Starting three-layer models, where resistivity decreases with depth, were used in this study to simulate apparent resistivity data measured in the field. Since the static water level is generally found at a few meters above mean sea level (MSL) in the coastal parts of the island, the thickness of the first layer was fixed (as a first approach) to place its lower boundary approximately at MSL. However, several sounding inversions (soundings N2–N5) required a shallow thin low-resistivity layer in the model in order to obtain an adequate fit to the data. Figure 2 shows the 1-D electrical models obtained from inversion of the data at typical sites N5, N8, and S1 in the form of the equivalent resistivity versus depth sections. As shown in Figure 2, the depth to the conductive basement at site N8 is almost uniquely determined. The depth may vary between 148 and 158 m, with the depth of 152 m obtained for the best fit model. At site S1 the depth to the basement is less well resolved, displaying a degree of variance, but the resistivity of the conductive layer is highly determined. At site N5 the intermediate thin conductive layer is only resolved by the conductance (resistivity between 12 and 27 ohm m and thickness in the range of 2–7 m).

AMT Soundings

The AMT method measures naturally occuring electromagnetic fields over a broad frequency range from 1 Hz to 10 kHz, which are used to give information on resistivity variations with depth [*Strangway et al.*, 1973]. In Grand Brulé (Figure 1) all measurements have been made with a tensor Iris Instruments SAMTEC2 system. The data from this study have been analyzed to produce, as a function of frequency at each sounding site, apparent resistivities and phases and E and H polarization (transverse electric (TE) and transverse magnetic (TM)) mode) orientations of the impedance tensor [*Vozoff*, 1972]. In 2-D models, TE and TM mode are aligned parallel and perpendicular to strike, respectively. In Figure 3 the TE and TM responses at typical sites S3 and N1 (Figure 1) are shown. The AMT response observed at site S3 is characterized by an abrupt decrease in resistivity with frequency, without any other prominent feature. This characteristic was found for most of AMT soundings except for sites close to the coast, where a flatting in the intermediate part of the curve occurs (for example results for typical site N1). In general, the small deviations between the TE and TM curves observed for most of AMT soundings (typical site S3, Figure 3) indicate that as a first approximation a 1-D modeling of the sounding curves can be considered. Some exceptions to the 1-D character can be seen at some sites, where a very pronounced parallel split occurs between the principal apparent resistivity curves (particularly at site N4) at all frequencies. This distortion of the soundings is attributed to local superficial heterogeneities. This is commonly referred to as static shift [*Berdichevsky and Dmitriev*, 1976; *Jiracek*, 1990]. Interpretations based on these data will be erroneous. This distortion is seen only on the amplitude data, and the phase data are unaffected. Methods of correcting static shift require information about the continuity of deep structure [*Jones*, 1988] and/or measurements of shallow structure by

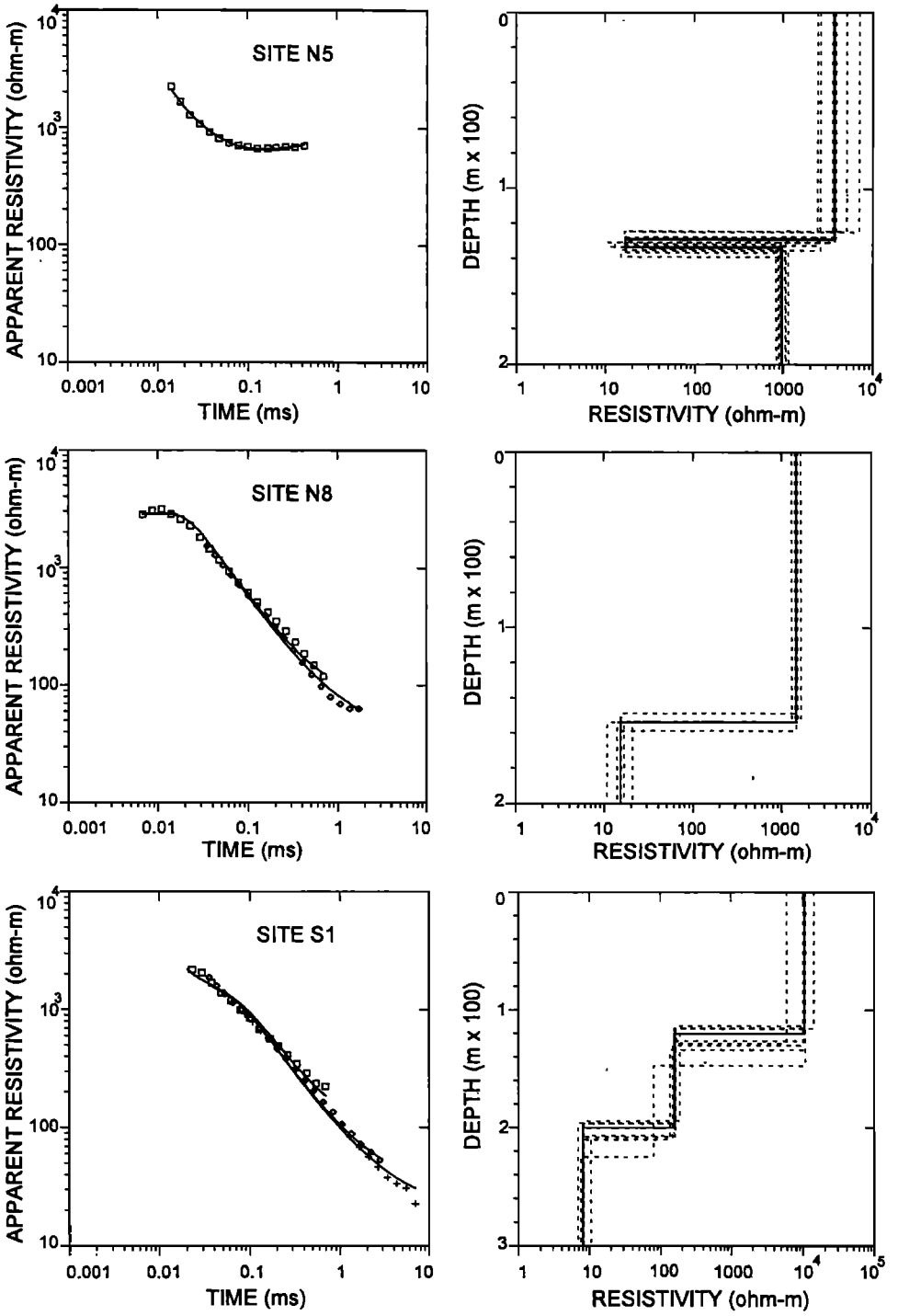

Figure 2. Examples of TDEM sounding curves at typical sites N5, N8, and S1 (Figure 1). Symbols in the left-hand graph represent three-frequency field data. Solid lines (in the left-hand graph) represent three-frequency calculated responses for the best fit models shown in the right-hand graph. Dashed lines are the equivalent models. At sites N5 and S1, late-time data are rejected because the signal appeared to be noisy.

inductive controlled source electromagnetic methods [*Sternberg et al.*, 1988; *Pellerin and Hohmann*, 1990]. To correct this shift, we have utilized the procedure of *Pellerin and Hohmann* [1990] based on 1-D TDEM inversion. For example, from the TDEM model at site N4, an AMT sounding curve is computed within the period of AMT and TDEM overlap (frequencies above 300 Hz and higher). It appears that all three curves have the same shape and are parallel. The TDEM apparent resistivity curve agreed closely with the AMT maximum amplitude curve, and this one should be used to obtain a much more accurate picture of the resistivity structure at depth.

Strong lateral changes in surface resistivity change the electromagnetic field considerably. For example, the effect of the ocean shore is well known [e.g., *Ogawa*, 1987]. However, for

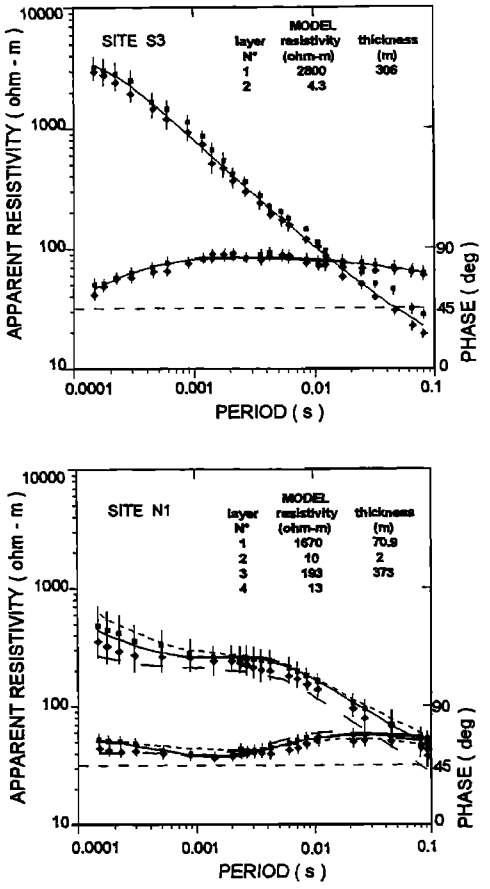

Figure 3. Examples of AMT soundings for sites N1 and S3 (Figure 1). Solid squares and diamonds with errors bars (95% confidence intervals, not plotted when smaller than the symbols) denote the observed values for TM and TE mode, respectively. Solid lines represent the fit obtained with one dimensional (1-D) models. The upper part of the model for sounding N1 is obtained from the results of the TDEM interpretation. At site N1, short- and long-dashed lines are transverse magnetic and transverse electric mode responses, respectively, determined from a 2-D model with an ocean (see text).

soundings more than 1–2 skin depths from the boundary, the ocean has a minor effect. In the study area the soundings N1, N2, and S1 close to the coast can be influenced by the coastal effect. Site N1 is less than 500 m from the ocean, and the skin depth at 100 Hz is about 500 m assuming the resistivity of 100 ohm m. An assessment of the coastal effect has been made from 2-D models [*Wannamaker et al.*, 1987]. We started 2-D modeling with only the shallow resistivity and depth features referring to the preliminary 1-D result [*Jupp and Vozoff*, 1975] at site N1 close to the coast (Figure 1), including topography [*Wannamaker et al.*, 1986] but no ocean. The AMT responses of TM and TE mode were calculated and compared with the field values along profile N. For example at site N1, topographic responses for both modes appear nonanomalous (isotropic) across the observational bandwidth (a 1-D interpretation is appropriate) and are within the error bars of the field data (Figure 3). Errors are generally within 22% for the apparent resistivities and within 8% for the phase. In Figure 3, topographic responses were omitted for clarity. To see the coastal effect in AMT data, responses for the initial 2-D model with a conductive ocean (0.3 ohm m) were calculated. Site N1 (Figure 3) shows a significant amount of shift between the TM and TE calculated amplitude curves across the entire bandwidth. However, the TM calculated responses from models with and no ocean are very similar and are within the confidence limits of the observed values for TM mode. Consequently, for a first-order approximation, the effect of the ocean in the TM mode data above 10 Hz can be neglected. The ocean has a major effect in TE mode. At site N2, coastal effect is much more weakened and appears at frequencies below 30 Hz for TE mode. For the remainder of the sites a contribution from the ocean can be neglected above 10 Hz.

On the basis of these analyses, 1-D inversion [*Jupp and Vozoff*, 1975] was employed to fit the AMT data. At sites N1, N2, and S1 close to the coast the TM mode data have been emphasized in the modeling process because they are more immune to coastal effects in the area than are the TE mode data, as discussed above. We used the TDEM models as constraints on the shallow structure to produce AMT results that are similar to the field measurements. The inferred resistivity structures by 1-D inversion at each site are then pieced together to produce a cross section along two profiles. Typical field data and synthetic data from 1-D inversion are shown in Figure 3. Our constraints based upon interpretation of TDEM data may be erroneous; however, we are confident that these are realistic because the results from completely different electrical methods match. The cross section for profile N (Figure 4) indicates the following resistivity properties of the northern edge of Grand Brulé: (1) a resistive surface layer 70–400 m thick that can be locally subdivided into two units for coastal soundings (sites N1–N5), where additional conductive layers of less than 20 ohm m, 5–10 m thick appear in the interior of the resistive layer, (2) an intermittent second layer of intermediate resistivity values of about 200 ohm m, 200–400 m thick. This layer becomes less thick as one goes farther away from the coast, and a discontinuity, possibly a major fault or an unconformity is suggested between sites N4 and N6, as evidenced by the disappearance of this intermediate resistivity layer east of site N6, and (3) a low-resistivity third layer (8–15 ohm m). The top of this conductor has an irregular form and dips eastward. The resistivity structure deduced for the southern edge of Grand Brulé is much simpler than that for the northern edge. Our interpretation indicates that the study area can be broadly divided into two geoelectric regions: the summit area and the coastal area. The summit area consists of two layers whose resistivities vary from more than 2000 ohm m at the surface to 10 ohm m or less at depths of about 300 m. Beneath the coastal area, a 120–200 ohm m layer is sandwiched between a high-resistivity layer above and a low-resistivity layer below.

Comparison With Well Information

As seen in Figure 1, two wells [*Gérard and Rançon*, 1981; *Rançon et al.*, 1989] have been drilled in Grand Brulé (GB), but only lithologic logs based upon cuttings (sampled every 5 m) and cores exist. No information is available about the depth of the water table. At GB (3 km deep) the temperature does not show any significant gradients above a depth of about 480 m, where high porosities and permeabilities occur in the subaerial basaltic flows. At Vierge au Parasol (VP) (235 m deep) there is no significant decrease in porosity with depth.

Comparison between the lithologic log from VP (Figure 5) and layered resistivity sounding interpretation from site N1

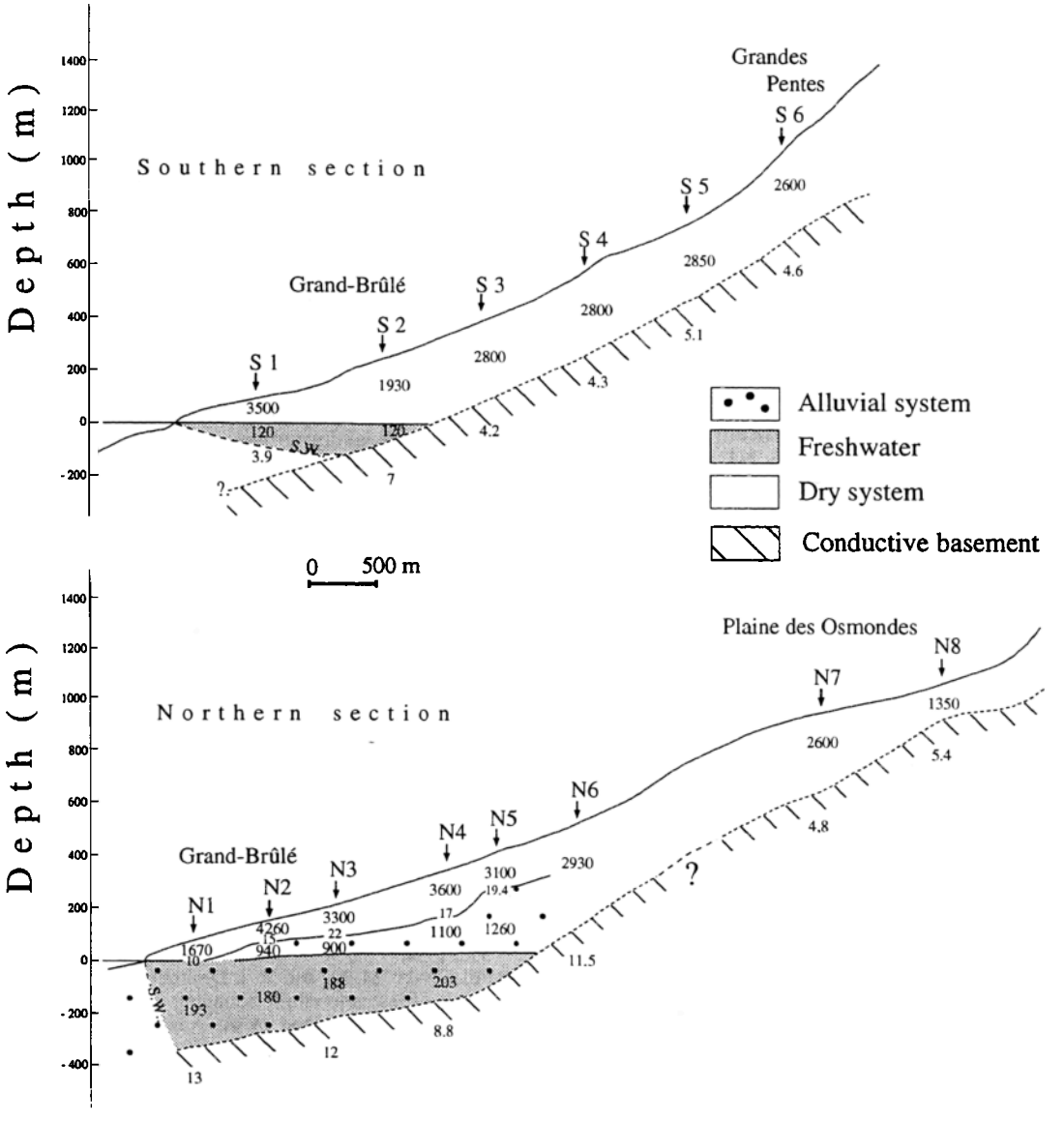

Figure 4. Composite geoelectrical 1-D cross sections along two profiles N and S (Figure 1) obtained from the combination of TDEM and AMT data. The numbers are interpreted resistivities in ohm meters. The first-layer resistivities were determined from TDEM data. The interrupted solid line indicates the positions of conductive discontinuities as seen by the EM47 system. The intermediate resistivities (120–200 ohm m) were determined by AMT data. An interpretation of the inferred resistivity structure is also shown. SW is the saltwater wedge.

(650 m from VP) shows a correspondence between the subaerial basaltic surface flows and the resistive (1670 ohm m) first layer. The transition to the alluvial deposits is marked by a 2-m-thick layer with a minimum resistivity of 10 ohm m which is not present in the VP log. The 193 ohm m unit is related to the sequence of basaltic materials with many alluvial beds.

The lithologic log from GB (Figure 5) is compared to the modeling results at site N2, located about 900 m to the south. The upper resistive layer (4260 ohm m) coincides with the subaerial basaltic flows. The top of the low-resistivity unit (8.5 ohm m) in depth roughly coincides with a lithologic boundary, namely with the top of the transitional sequence characterized by intercalation of subaerial and submarine flows and the presence of coastal deposits. The 940 ohm m unit at site N2 is not present in the GB log.

Discussion

On the basis of the well VP and GB log information, possible explanations for the difference between the resistivities of the different layers (Figure 4) are the degree of fluid saturation, pore fluid resistivity, and presence of clays. For profile N and S (Figure 4), resistivities in excess of 900 ohm m probably represent dry or slightly wetted basaltic materials. In the some parts of the cross section N, mainly in the eastern half, intercalated intermittent thin low-resistivity layers occur within lava flows and might be due to the prevalence of argilized interbeded lahars.

The intermediate resistivities (120–200 ohm m) are too low for dry basaltic rocks and can be interpreted in terms of freshwater saturation in the second layer. Correlation with well VP

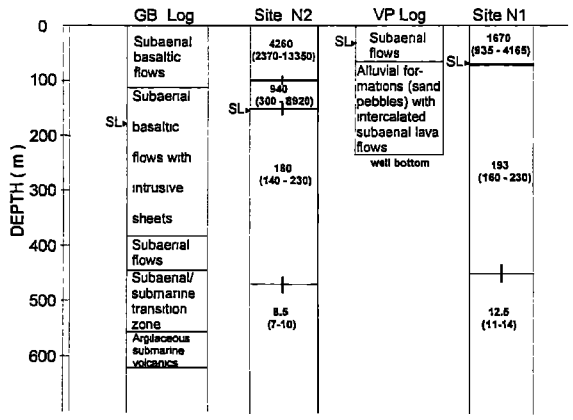

Figure 5. Comparison of the geophysically determined layers from the AMT/TDEM data at sites N1 and N2 with drill hole sections at VP and GB, respectively. In the geoelectrical models the heavy horizontal line represents a thin conductive (about 10 ohm m) layer. Numbers are the interpreted resistivities in ohm meters. Acceptable resistivities are indicated by values in parentheses. The error bars on the layer boundaries are 95% confidence intervals (not shown when smaller than the line thickness). SL is the sea level.

log information shows that this aquifer is composed of alluvial formations. The high-/intermediate-resistivity interface is generally found at about MSL (sites N1–N4 and S1–S2).

The deeper layer is characterized by resistivities of less than 15 ohm m, which points to clayed zones or a higher groundwater salinity or both. The persistence of low resistivities from the coast to farther inland in high areas where the conductor top rises to greater than 800 m above sea level is best explained by clayed zones. Near the coast, however, seawater intrusion cannot be ruled out as the cause of the low resistivities because depths to the conductive layer are BSL. In the absence of additional supporting information we assume that the conductor may be the manifestation of a clayey, poorly permeable base, probably containing saline water near the coast.

A comparative analysis of the two profiles N and S underlines the complex electrical structure of the Grand Brulé/Plaine des Osmondes area. Profile S is quite simple, and a coherent geological interpretation can be proposed up to 300-m elevation. A resistive layer of recent lava flows with high porosity overlies a very conductive basement of unknown thickness. The top of this basement may be the upper part of a layer of mixed, crushed argillized basaltic materials produced by a huge landslide on the volcano flank. Freshwater above this relatively impermeable layer lies upon the seawater near the coast with a typical landward low-dipping interface and forms a third freshwater saturated interbedded basaltic layer of intermediate resistivity. If the upper part of profile N (sites N7 and N8) resembles profile S with resistive lava flows overlying a conductive layer, its lower part shows a five-layer geoelectrical model (sites N1–N4). However, well VP (near site N1) has delivered crucial information, namely that below 60 m of recent lava flows, alluvial deposits were found down to 170 m BSL. The thick (>300 m) layer of intermediate (~200 ohm m) resistivity found at site N1 is then probably related to this alluvial fan. Its geophysical continuity inland suggests a paleoalluvial system up to the Plaine des Osmondes area. The thickness of this layer and its present location BSL may be explained by contemporaneous or late seaward collapse of Grand Brulé during the paleoriver formation. The observed resistivity jump from 800–1200 ohm m to 180–200 ohm m near MSL is clearly related to the water table with a contact between dry and freshwater saturated alluvium.

Conclusions

The TDEM/AMT survey has proven to be particularly effective for defining the shallow geoelectrical structure of a volcanic body and the aquifer system developed in it. Such measurements may be used to locate large bodies of groundwater with anomalous electrical properties. Grand Brulé resistivity survey on its northern edge suggests the presence of a previously unknown thick aquifer below sea level, which contains freshwater even near the coast. This aquifer can be related to alluvial formations revealed by a borehole near the coast. Its geophysical continuity landward is interpreted as a major paleoalluvial system buried under recent lava flows. This subsurface drainage structure likely obtains its recharge from precipitation in the Plaine des Osmondes and Enclos Fouqué areas (Figure 1).

Acknowledgments. This work was supported by a Conseil Général de la Réunion research grant in the framework of Fournaise Massif Hydrogeological Program directed by J. Coudray. We are grateful to Y. Albouy, P. Mourgues, and J. Descloitres for their field contributions. The writers also thank J. Kauahikaua and an anonymous reviewer for critical reviews and many useful suggestions on the manuscript.

References

Benderitter, Y., and A. Gérard, Geothermal study of Réunion Island audiomagnetotelluric survey, *J. Volcanol. Geotherm. Res.*, *20*, 311–332, 1984.

Berdichevsky, M. N., and V. I. Dmitriev, Basic principles of interpretation of magnetotelluric sounding curves, in *Geoelectric and Geothermal Studies*, edited by A. Adam, pp. 163–221, Akad. Kiado, Budapest, 1976.

Chevallier, L., and P. Bachèlery, Evolution structurale du volcan actif du Piton de la Fournaise, Ile de la Réunion, Océan Indien, *Bull. Volcanol.*, *45*, 287–298, 1981.

Duffield, W. A., L. Stieltjes, and J. Varet, Huge landslide blocks in the growth of Piton de la Fournaise, La Réunion, and Kilauea volcano, Hawaii, *J. Volcanol. Geotherm. Res.*, *12*, 14–160, 1982.

Eaton, P. A., and G. W. Hohmann, An evaluation of electromagnetic methods in the presence of geologic noise, *Geophysics*, *52*, 1106–1126, 1987.

Fitterman, D. V., and M. T. Stewart, Transient electromagnetic sounding for groundwater, *Geophysics*, *51*, 995–1005, 1986.

Gérard A., and J. P. Rançon, Évaluation du potential géothermique de l'île de la Réunion, Étude détaillée du site du Grand-Brûlé, *Rep. BRGM-81SGN669GTH*, 13 pp., Bur. de Rech. Geol. et Minières, Orléans, France, 1981.

Jiracek, G. R., Near-surface and topographic distortions in electromagnetic induction, *Surv. Geophys.*, *11*, 163–203, 1990.

Jones, A. G., Static-shift of magnetotelluric data and its removal in a sedimentary basin environment, *Geophysics*, *53*, 967–978, 1988.

Jupp, D. L. B., and K. Vozoff, Stable iterative methods for the inversions of geophysical data, *Geophys. J. R. Astron. Soc.*, *50*, 333–352, 1975.

Kaufman, A. A., and G. R. Keller, *Frequency and Transient Sounding*, 685 pp., Elsevier, New York, 1983.

Keller, G. R., and F. C. Frischknecht, *Electrical Methods in Geophysical Prospecting*, Pergamon, Tarrytown, N. Y., 1966.

Lénat, J. F., P. Vincent, and P. Bachèlery, Sea-beam mapping of the offshore continuation of an active basaltic volcano: Piton de la Fournaise (Reunion Island, Indian Ocean), structural and geomorphological interpretation, *J. Volcanol. Geotherm. Res.*, *36*, 1–36, 1989.

Ogawa, Y., Two-dimensional resistivity modeling based on regional

magnetotelluric survey in the northern Tohoku district, northeastern Japan, *J. Geomagn. Geoelectr.*, *39*, 349–366, 1987.

Pellerin, L., and G. W. Hohmann, Transient electromagnetic inversion: A remedy for magnetotelluric static shifts, *Geophysics*, *55*, 1242–1250, 1990.

Rançon, J. P., P. Lerebour, and T. Augé, The Grand Brulé exploration drilling: New data on the deep framework of the Piton de la Fournaise volcano, 1, Lithostratigraphic units and volcano structural implications, *J. Volcanol. Geotherm. Res.*, *36*, 113–127, 1989.

Sternberg, B. K., J. C. Washburne, and L. Pellerin, Correction for the static shift in magnetotellurics using transient electromagnetic soundings, *Geophysics*, *53*, 1459–1468, 1988.

Strangway, D. W., C. M. Swift, and R. C. Holmes, The application of audio-frequency magnetotelluric (AMT) to mineral exploration, *Geophysics*, *38*, 1159–1175, 1973.

Vozoff, K., The magnetotelluric method in the exploration of sedimentary basins, *Geophysics*, *37*, 98–141, 1972.

Wannamaker, P. E., J. A. Stodt, and L. Rijo, Two-dimensional topographic responses in magnetotellurics modeled using finite elements, *Geophysics*, *51*, 2131–2144, 1986.

Wannamaker, P. E., J.A. Stodt, and L. Rijo, A stable finite element solution for two-dimensional magnetotelluric modeling, *Geophys. J. R. Astron. Soc.*, *88*, 277–296, 1987.

M. Courteaud and B. Robineau, Laboratoire des Sciences de la Terre, Université de la Réunion, BP 7151, 97715 St-Denis messag cedex 9, Ile de la Reunion, France.

M. Descloitres and M. Ritz, Institut Français de Recherche Scientifique pour le Developpement en Coopération, BP 1386, Dakar, Senegal. (e-mail: descloit@dakar.orstom.sn)

(Received July 11, 1995; revised August 13, 1996;
accepted August 28, 1996.)